

## Research Article

# Ceramide and Related-Sphingolipid Levels Are Not Altered in Disease-Associated Brain Regions of APP<sup>SL</sup> and APP<sup>SL</sup>/PS1<sup>M146L</sup> Mouse Models of Alzheimer's Disease: Relationship with the Lack of Neurodegeneration?

Laurence Barrier, Bernard Fauconneau, Anastasia Noël, and Sabrina Ingrand

*Groupe de Recherche sur le Vieillissement Cérébral, GreViC EA 3808, Faculté de Médecine et de Pharmacie, 6 rue de la Milétrie, BP 199, 86034 Poitiers Cedex, France*

Correspondence should be addressed to Laurence Barrier, lbarrier@univ-poitiers.fr

Received 27 September 2010; Accepted 16 November 2010

Academic Editor: J. Fantini

Copyright © 2011 Laurence Barrier et al. This is an open access article distributed under the Creative Commons Attribution License, which permits unrestricted use, distribution, and reproduction in any medium, provided the original work is properly cited.

There is evidence linking sphingolipid abnormalities, APP processing, and neuronal death in Alzheimer's disease (AD). We previously reported a strong elevation of ceramide levels in the brain of the APP<sup>SL</sup>/PS1Ki mouse model of AD, preceding the neuronal death. To extend these findings, we analyzed ceramide and related-sphingolipid contents in brain from two other mouse models (i.e., APP<sup>SL</sup> and APP<sup>SL</sup>/PS1<sup>M146L</sup>) in which the time-course of pathology is closer to that seen in most currently available models. Conversely to our previous work, ceramides did not accumulate in disease-associated brain regions (cortex and hippocampus) from both models. However, the APP<sup>SL</sup>/PS1Ki model is unique for its drastic neuronal loss coinciding with strong accumulation of neurotoxic A $\beta$  isoforms, not observed in other animal models of AD. Since there are neither neuronal loss nor toxic A $\beta$  species accumulation in APP<sup>SL</sup> mice, we hypothesized that it might explain the lack of ceramide accumulation, at least in this model.

## 1. Introduction

Alzheimer's disease (AD) is the most common form of dementia in adults. Pathologically, the hallmarks of AD are amyloid plaques and neurofibrillary tangles, associated with widespread neuronal loss. Its fundamental causes and the pathological cascades leading to symptoms, however, remain poorly understood. Lipids and lipid peroxidation products have important roles in central nervous system homeostasis. Extensive evidence supports an important role of cholesterol in the development and possibly progression of AD [1–3]. The role of other lipids, such as ceramides and related-sphingolipids, (sphingomyelins, sulfatides, and glycosphingolipids) is also emerging. Ceramides are the core constituent of most sphingolipids. They can be produced by hydrolysis of sphingomyelin (SM) via sphingomyelinases (SMases) or synthesized de novo from fatty acyl CoA and sphingosine. Conversely, in the Golgi, ceramides may be transformed

into SM by the addition of phosphorylcholine. Additionally, glycosyltransferases can attach sugar to ceramide, turning it into glucosylceramide or galactosylceramide (Galcer), a key step in the generation of complex glycosphingolipids [4, 5].

Ceramides are important second messenger molecules that regulate diverse cellular processes including cell growth, differentiation, and apoptosis. Ceramide levels also increase in response to aging and various age-related stress factors and are directly involved in apoptotic signaling in various cell types, including neurons [6–8].

There is evidence linking sphingolipid abnormalities, APP processing, and neuronal death in AD. In vitro, it has been shown that  $\beta$ -amyloid added to cultured neurons [9, 10] or oligodendrocytes [11] increase SMase activity, leading to an increase in ceramide levels [12]. Additional reports have found that ceramide levels increase  $\beta$ -amyloid synthesis [12, 13] and favor gamma secretase processing of APP [14–16] so that inhibition of ceramide synthesis

confers protection against  $\beta$ -amyloid [9]. Thus, it has been suggested that ceramides and  $\beta$ -amyloid may synergize to induce neuronal death.

Several studies have examined the sphingolipid alterations in human AD brain. For example, the total phospholipid and sulfatide content in AD was decreased as compared to normal [17–19], while the ceramide and galactosylceramide levels were elevated [9, 18]. Enhanced ceramide levels have been reported in the cerebrospinal fluid (CSF) of patients with AD [20] and changes in the activity of several key enzymes of ceramide metabolism, in gene expression of pathways associated to sphingolipid metabolism have been found in brains of AD patients [21, 22].

During the last years, numerous mouse transgenic lines have been created and have been screened for various aspects of AD pathology [23, 24]. Unfortunately, very little work has been done on determining if sphingolipid content is likewise perturbed in these rodent models of AD. In one study, long-chain ceramides were shown to be elevated in presenilin 1 (PS1M146V) mouse brain and to induce apoptosis in PS1 astrocytes [25]. In a second study, sulfatides, a class of sulfated galactocerebrosides, were found to be decreased in brain tissues from two APP transgenic mice (i.e., APPV717F and APPsw), whereas no significant changes in the content of other sphingolipid classes including SM, Galcer, and ceramides were noted [26]. By contrast, using the new mouse mutant APP<sup>SL</sup>/PS1Knock-in line, we have recently found an early and significant increase of ceramides in the cortex of these mice, without significant changes in other sphingolipid levels [27]. However, the APP<sup>SL</sup>/PS1Ki model is unique for its drastic neuronal loss, not observed in other animal models of AD [28]. The discrepancy in the few data available and the lack of knowledge of sphingolipid levels in the brain of other rodent models of AD prompted us to investigate whether the sphingolipid composition is altered in the brain of two other mouse models of AD: single APP<sup>SL</sup> and double APP<sup>SL</sup>/PS1<sup>M146L</sup> transgenics. Concentrations of ceramides, SM, Galcer, and sulfatides were determined in three brain regions: the cortex and the hippocampus, the two brain regions typically associated with the disease, and the cerebellum, a nonvulnerable region with no A $\beta$  plaques. For all analyses, age-matched PS1<sup>M146L</sup> (amyloid free) mice as well as nontransgenic wild-type mice (WT) were used.

## 2. Materials and Methods

**2.1. Chemicals.** All organic solvents were of analytical grade and came from VWR International (Strasbourg, France). HPTLC-plates Silicagel 60, 10  $\times$  10- or 10  $\times$  20 cm were purchased from Merck (VWR International). Lipid standards (nonhydroxy fatty acid (NFA) containing ceramides, ceramides containing 2-hydroxy fatty acids (2-HFA), sphingomyelins, cerebroside sulfate (sulfatides), and galactosylceramides (a mixture containing 2-hydroxy fatty acids and nonhydroxy fatty acids) were purchased from Sigma-Aldrich (France). Aminopropyl-bonded (LC-NH<sub>2</sub>) silica gel cartridges (100 mg matrix) were from Supelco (Saint Quentin Fallavier, France).

**2.2. Transgenic Mice.** Generation and detailed neuropathological analyses of the APP<sup>SL</sup> and the APP<sup>SL</sup>/PS1<sup>M146L</sup> transgenic mice have been described earlier [29, 30]. In brief, these mice express human APP751 with Swedish and London mutations (Thy1 promoter) either alone or in combination with human presenilin-1 (M146L, HMG-CoA promoter). In this study, 12-month-old ( $n = 5$ ) APP<sup>SL</sup>/PS1<sup>M146L</sup> double transgenic, 12-month-old ( $n = 5$ ) PS1<sup>M146L</sup> single-transgenic littermates, and 12-month-old ( $n = 6$ ) nontransgenic mice as well as 24 month-old ( $n = 5$ ) APP<sup>SL</sup> single transgenic and 24-months ( $n = 5$ ) nontransgenic littermates were used (generous gift of Sanofi-Aventis, Vitry sur Seine, France). APP<sup>SL</sup> mice were analyzed at 24 months of age and APP<sup>SL</sup>/PS1<sup>M146L</sup> mice were assessed at 12 months of age because they revealed comparable levels of amyloid plaques in the brain at these respective ages. The genetic background of the mice was mixed CBA/C57BL/6. All the mice used in this study were female, because a gender effect with female mice displaying more severe pathology than male has been mentioned in several studies [27, 31, 32].

All experiments were performed in compliance and following approval of the Sanofi-Aventis Animal Care and Use Committee and in accordance with standards of the guide for the care and use of laboratory animals (CNRS ILAR) and with respect to French and European Community rules.

**2.3. Brain Tissue Preparation.** The mice were anesthetized with pentobarbital (40 mg/kg, IP) and sacrificed. Brains were removed immediately, and cortex, hippocampus, and cerebellum were dissected. These cerebral regions were homogenized by 10 up-and-down strokes of a prechilled Teflon-glass homogenizer in 20 volumes of buffer (25 mM Tris-HCl, 150 mM NaCl, 1 mM EDTA, pH 7.4) and supplemented with 50 mM sodium fluoride, 1 mM phenylmethylsulfonyl fluoride, protease, and phosphatase inhibitor cocktails (50  $\mu$ L/g tissue and 10  $\mu$ L/mL lysis buffer, resp.). The homogenates were centrifuged at 15,000 g for 15 min at 4°C. The resulting pellet was resuspended in 3 volumes of ice-cold water, altogether 1.5 mL, homogenized at 4°C (10–15 strokes) and then sonicated for 20 s using a sonifier (Branson Ultrasonics, sonifier 450, Danbury, CT). Samples from each mouse brain were analyzed separately and in duplicate.

**2.4. Lipid Extraction from Tissues and Thin-Layer Chromatography.** Total lipids from brain homogenates were prepared according to previously described procedures [27, 33]. Briefly, the homogenates were added to 8 vol. of rapidly stirring methanol, then 4 vol. of chloroform were added. The mixture was stirred overnight, and then centrifuged at 1,000 g for 10 min. The pellet was re-extracted with chloroform-methanol-water (4:8:3, v/v/v) and the two supernatants combined, evaporated to dryness. Partitioning was carried out using diisopropyl ether/1-butanol/50 mM aqueous NaCl (6:4:5, v/v/v) according to the method of Ladisch and Gillard [34]. The total upper phase was evaporated to dryness and taken up in chloroform. The lipids were fractionated using solid-phase extraction on

100 mg LC-NH<sub>2</sub> cartridges (Supelco, L'Isle d'Abeau, France) as previously described [27]. The eluted fractions containing, respectively, free ceramides, galactosylceramides (Galcer), alkali-stable phospholipids (SM), and sulfatides were applied to HPTLC plates with a Linomat 5 (Camag, Switzerland). Prior to SM analysis, the phospholipid-containing fraction was subjected to mild alkaline methanolysis (treatment with chloroform: 0.6 N NaOH in methanol 1:1 (v/v) at room temperature for 1 h) to remove glycerophospholipids. To quantify each lipid species (ceramides, SM, Galcer, and sulfatides), calibration curves were obtained by running in parallel known amounts of purified lipid standards. For free ceramides, 15–20 mg of brain tissue (wet weight) was spotted per lane. The plates were developed with chloroform-methanol 50:3 (v/v) and visualized by charring for 10 min at 180°C with 3% cupric acetate in 8% phosphoric acid solution. For SM analysis, 6–9 mg of tissue was spotted per lane. The plates were developed with chloroform-methanol-water 60:35:8 (v/v/v). SM was visualized with sulfuric acid-CuSO<sub>4</sub>-ammonium molybdate spray reagent followed by heating at 110°C for 15 min. Galcer and sulfatides (about 0.4 mg and 2 mg of tissue per lane, resp.) were developed in chloroform-methanol-water 65:25:4 (v/v/v), sprayed with orcinol-H<sub>2</sub>SO<sub>4</sub> reagent, and then heated at 150°C for 2 min.

Each sphingolipid species was quantified by scanning densitometry of the plates at 396 nm for ceramides, 540 nm for Galcer and sulfatides, and 750 nm for SM with the Camag TLC Scanner 3/WinCats software system.

**2.5. Statistical Analysis.** The results were presented as mean  $\pm$  S.D. values. Owing to the small number of animals per group, statistical analysis of the data was performed using a nonparametric Kruskal-Wallis test followed by a posthoc test of Dunn for multiple comparisons. For the comparison of two means, the Mann-Whitney test was used. All calculations were performed using GraphPad Prism software 3.02 (GraphPad Software, Inc.). *P* values less than .05 were considered as significant.

### 3. Results

In single APP<sup>SL</sup> mice (Figure 1(a)), a moderate but not significant elevation of NFA-ceramides was seen in the cortex (+22%), with no changes of the 2-HFA-ceramide level. Conversely, in the hippocampus (Figure 1(b)), the NFA-ceramide level did not differ between WT and APP<sup>SL</sup> mice, whereas a tendency towards an increase of 2-HFA-ceramides was noted (+19%), although it was not significant.

Surprisingly, as shown in Figure 1(c), the level of 2-HFA-ceramides in the cerebellum of APP<sup>SL</sup> mice was significantly increased in comparison to the counterpart of their WT littermates (+50%, *P* < .05). Conversely, the NFA-ceramides showed a slight but not significant decrease compared to WT control values. However, no difference in the total ceramide content was noticed in the cerebellum of both WT (51.35  $\pm$  1.45 nmol/mg tissue) and APP<sup>SL</sup> mice (50.28  $\pm$  3.31 nmol/mg tissue).

Because the double-transgenic mouse model APP<sup>SL</sup>/PS1<sup>M146L</sup> develops neuropathological features of AD earlier than the single APP<sup>SL</sup> mice [29], the sphingolipid analysis was performed in the brain regions of this model in younger animals (12 months of age). As shown in Figures 2(a) and 2(b), concentrations of NFA-ceramides as well as those of 2-HFA-ceramides did not differ between wild-type, PS1<sup>M146L</sup>, and APP<sup>SL</sup>/PS1<sup>M146L</sup> mice in the two disease-associated brain regions (cortex and hippocampus). In contrast to the changes of ceramide content in cerebellum of APP<sup>SL</sup> mice, the NFA-ceramide as well as the 2-HFA-ceramide levels were unchanged in this brain region in APP<sup>SL</sup>/PS1<sup>M146L</sup> mice relative to their WT controls and PS1 littermates (Figure 2(c)). However, NFA-ceramide content showed a tendency towards a decrease, while 2-HFA ceramides tended to slightly increase in the cerebellum of the APP<sup>SL</sup>/PS1<sup>M146L</sup> mice.

It should be noted that, although cortex and hippocampus of WT mice displayed almost identical ceramide content (Figures 1(a), 1(b), 2(a), and 2(b)), a relatively lower NFA-ceramide content was manifest in the cerebellum (Figures 1(c) and 2(c)). In normal human brain, the ceramide levels were also reported much higher in the cortex versus the cerebellum [18].

Typical ceramide profiles from either cortex, hippocampus, or cerebellum of the different transgenic mice and wild-type controls were shown in Figure 3. Since 2-HFA-ceramides are present in extremely low levels leading to a weak staining on the HPTLC plate, densitometric scanning of the plate was shown to visualize the peak corresponding to the 2-HFA-ceramide species (Figure 3).

To test whether other related-sphingolipids could be altered in the brain of transgenic mice, the content of SM, Galcer, and sulfatides in lipid extracts of the three examined brain regions was assessed by HPTLC analysis. Figures 1(d)–1(f) show that sphingolipids (SM, Galcer, and sulfatides) did not display significant changes in both cortex, hippocampus, and cerebellum of APP<sup>SL</sup> mice compared to the WT littermates. Similarly, the levels of SM, Galcer, and sulfatides did not differ among nontransgenic, PS1<sup>M146L</sup> and APP<sup>SL</sup>/PS1<sup>M146L</sup> mice in all brain region examined (Figures 2(d)–2(f)). It should be noted that there are differences of SM, Galcer, and sulfatide concentrations between cerebral tissues (cortex and hippocampus) and cerebellar tissues. In both models, cerebellum displayed higher levels of Galcer and sulfatides than cerebral tissues. This is in accordance with Cheng et al. [26] who also reported a ~2-fold higher level of sulfatides in the cerebellum compared to the cortex, in two other transgenic mouse models of AD. In contrast, SM levels were almost identical in hippocampus and cerebellum, but higher than those of cerebral cortex (Figures 1(d)–1(f) and 2(d)–2(f)). Examples of HPTLC profiles of sulfatides, Galcer, and SM and from either cortex, hippocampus, or cerebellum were represented in Figures 4(a), 4(b), and 4(c), respectively. It should be mentioned that the HPTLC profiles of each sphingolipid class were similar in all examined brain regions from both mouse models.

#### 4. Discussion

Using the same methodology as in our previous work [27], we herein analysed the sphingolipid composition of two additional models (i.e., single APP<sup>SL</sup> and double APP<sup>SL</sup>/PS1<sup>M146L</sup> mice) in which the time-course of pathology is much closer to that seen in the majority of currently available models. The main results of this study are (1) a moderate but not significant increase of NFA-ceramides and 2-HFA-ceramides in the cortex and the hippocampus respectively, of the APP<sup>SL</sup> mice, (2) unaltered ceramide levels in the two disease-associated brain regions from APP<sup>SL</sup>/PS1<sup>M146L</sup> mice, (3) unexpected alterations of the ceramide profile in the cerebellum of APP<sup>SL</sup> mice, a region with no A $\beta$  pathology, and (4) no significant changes in the other related-sphingolipids in all brain structures examined of both transgenic models. Based on our results and those from the literature, we will first discuss the possibility of a relationship between neurodegeneration, toxic A $\beta$  accumulation, and ceramide content. For the second time, why an amyloid-free brain region such as cerebellum showed ceramide alterations is discussed.

Ceramides were shown to accumulate in AD human brain regions and their levels vary by disease severity suggesting that they could be indicators of AD progression [9, 18, 35]. Similarly to what happens in human AD, we previously found that ceramides increase very early in the cortex of the APP<sup>SL</sup>/PS1Ki mouse model, preceding the neuronal loss [27]. By contrast, our present results reveal that in single APP<sup>SL</sup> mice, ceramide levels were not significantly altered in disease-associated brain regions (e.g., hippocampus or cortex). This is consistent with the findings of Cheng et al. [26] who reported no changes in ceramide content in any brain region from APP<sup>sw</sup> and APP<sup>V717F</sup> transgenic mice. An important difference between these single APP mouse lines and the APP<sup>SL</sup>/PS1Ki model is that the latter develops an early and massive neuronal loss which correlates with strong accumulation of intracellular A $\beta$ 42, A $\beta$  aggregates, and A $\beta$ 42 oligomers [28, 36]. Although intraneuronal A $\beta$  accumulation has also been documented in various APP models [29, 37, 38], a striking difference between the models used in the present study and the APP<sup>SL</sup>/PS1Ki mice is the nature of the A $\beta$  peptides which accumulate. Indeed, in APP<sup>SL</sup>/PS1Ki mouse brain, extremely high levels of N-truncated A $\beta$ x-42 variants and abundant oligomers were detected, which closely resembles that found in AD brain. By contrast, in APP<sup>SL</sup> mouse brain, with the same total A $\beta$  levels as in APP<sup>SL</sup>/PS1Ki mice, only very limited levels of A $\beta$ 42 N-terminal truncated isoforms were detected [28]. In the APP<sup>SL</sup>/PS1Ki mice, A $\beta$ x-42 is the major form accumulated with a ratio A $\beta$ x-42/total A $\beta$  close to 1. In comparison, this ratio is approximately of only 0.2-0.3 in the APP<sup>SL</sup> mice, and ~0.3-0.4 in the double transgenic APP<sup>SL</sup>/PS1<sup>M146L</sup> mice, similar to the range of values reported for a large number of other APP-based transgenics [28, 29].

N-truncated A $\beta$  peptides are known to aggregate more readily and are considered to be very toxic species. Thus they might play a key role in the neurotoxicity observed in the APP<sup>SL</sup>/PS1Ki model. In particular, the pyroglutamate

modified N-terminal truncated form of A $\beta$  at position 3 (A $\beta$ <sub>3(pE)-42</sub>), which represents a major species in the brain of AD patients [39], was recently shown to induce a severe neuron loss in the TBA2 mouse model, a new model expressing only N-truncated A $\beta$ <sub>3(pE)-42</sub> in neurons [40]. Interestingly, there is also a coincidence of considerable amounts of A $\beta$ <sub>3(pE)-42</sub> and massive neuron loss in the APP<sup>SL</sup>/PS1Ki mouse model [41]. On the basis of these findings, it is attractive to speculate that in APP<sup>SL</sup>/PS1Ki mice, the strong accumulation of intracellular toxic forms of A $\beta$  induces early elevation of ceramides. Extensive increase of ceramides could therefore activate proapoptotic pathways, leading to neuronal death. Conversely, other APP transgenic mouse models including the APP<sup>SL</sup> mice have been reported to show no [42] or very low A $\beta$ <sub>3(pE)-42</sub> levels [43]. This is due to the lack of posttranslational modifications such as N-terminal degradation and pyroglutamylation in these mice. Because APP<sup>SL</sup> mice display neither neuronal loss nor accumulation of highly toxic A $\beta$  42 isoforms, this may at least in part explain why no significant accumulation of ceramides occurred in the disease-associated brain regions of these mice.

Thus, despite numerous neuropathological, biochemical, and even behavioral changes representative of AD developed by these APP mice [23, 28–30, 33, 44], they may not constitute a relevant model to further explore the role of ceramides in AD pathology. However, answering the question of the relationship between neurodegeneration, toxic A $\beta$  accumulation, and ceramide elevation could be facilitated using restricted models either lacking (i.e., single APP mice) or mimicking only some specific AD-related neuropathological alterations (i.e., TBA2 mice mentioned above). Indeed, owing to the simultaneous occurrence of numerous pathological features of AD, the connection between them is often difficult to unravel.

We next determined the ceramide content in the double transgenic mouse model APP<sup>SL</sup>/PS1<sup>M146L</sup>, but in younger animals because the APP<sup>SL</sup>/PS1<sup>M146L</sup> mice develop neuropathological features of AD earlier than single APP<sup>SL</sup> mice [29]. At 12 months of age, these double transgenics revealed comparable levels of amyloid deposits than 24-month-old APP<sup>SL</sup> mice. Additionally, they displayed similar ganglioside alterations [33]. Our results showed that at 12 months of age, ceramide levels were unaltered in both cortex and hippocampus of APP<sup>SL</sup>/PS1<sup>M146L</sup> mice in comparison to age-matched PS1<sup>M146L</sup> mice and wild-type controls. It should be noted that there is no neuronal loss in these mice as old as 17 months, but unfortunately, older APP<sup>SL</sup>/PS1<sup>M146L</sup> mice were not available for this study. However, in our previous work, we demonstrated that elevation of ceramides occurred very early (3 months of age) in the cortex of the APP<sup>SL</sup>/PS1Ki model, preceding by far the neuronal loss detectable at 6 months of age. Why the APP<sup>SL</sup>/PS1Ki mice showed an increase of ceramides several months before the appearance of neuronal death while the APP<sup>SL</sup>/PS1<sup>M146L</sup> mice did not is currently unknown. One possible explanation is that the neuronal loss reported in the APP<sup>SL</sup>/PS1<sup>M146L</sup> mice is moderate and more restricted than in the APP<sup>SL</sup>/PS1Ki model. Indeed, the loss of neurons in the former involves

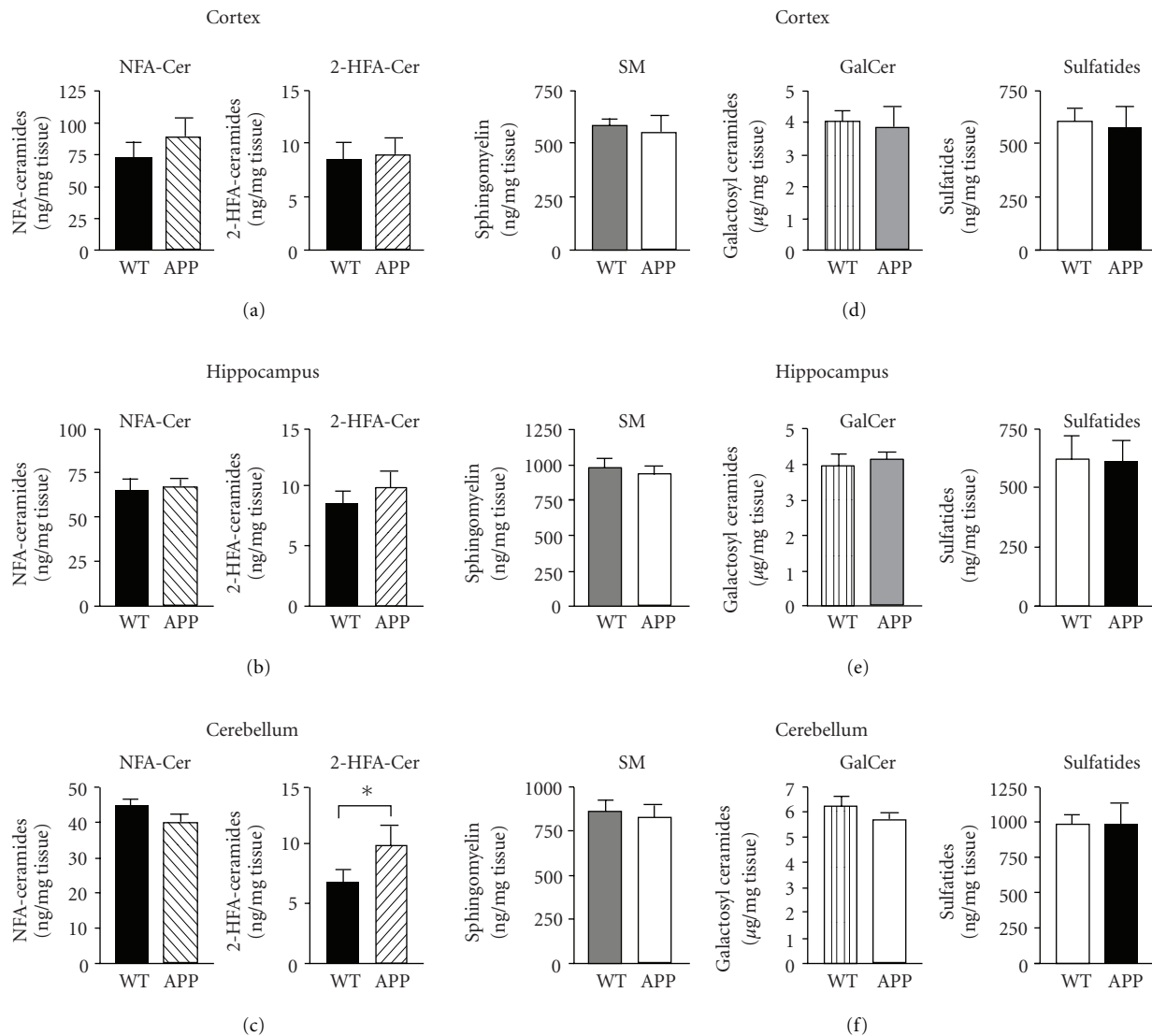


FIGURE 1: Levels of NFA-ceramides and 2-HFA-ceramides (a–c) and other related-sphingolipids (SM, GalCer, and sulfatides) (d–f) in the cortex, hippocampus, and cerebellum of 24-month-old APP<sup>SL</sup> mice and age-matched nontransgenic mice. WT: wild-type control mice. Each sphingolipid class was analyzed by HPTLC and their respective concentrations were calculated from standard curves after densitometric scanning of the plates as described under Section 2. Values are expressed as the means ± S.D. and statistically analyzed by a Mann-Whitney test. \* $P < .05$  compared to the respective wild-type mice.

only the hippocampal pyramidal cell layer (loss of ~30% in 17-month-old animals). This may in some way account for the lack of ceramide accumulation in the cortex of these mice. By comparison, in the APP<sup>SL</sup>/PS1Ki model, the cell loss is greater (~50% at 10 months of age) and has been shown to extend to other brain areas such as frontal cortex [36] and cholinergic system [45]. Moreover, as discussed above, accumulation of N-truncated A $\beta$  peptides should be lesser in APP<sup>SL</sup>/PS1<sup>M146L</sup> mice, since the ratio A $\beta$ <sub>x-42</sub>/total A $\beta$  is of 0.3 only, versus 1 in the APP<sup>SL</sup>/PS1Ki mice. In this context, it would seem likely that the level of highly toxic A $\beta$ <sub>3(pE)-42</sub> form, which is thought to be involved in neuronal death, is reduced in the APP<sup>SL</sup>/PS1<sup>M146L</sup> model. It is also possible that, at 12 months of age, it is too early to visualize an elevation of

ceramides, owing to the slowest progression of AD lesions in these mice than in the APP<sup>SL</sup>/PS1Ki model. Since we did not have older APP<sup>SL</sup>/PS1<sup>M146L</sup> mice, we should therefore be cautious to interpret the results of ceramide composition in these mice, because we cannot exclude the possibility that ceramides increase at a later age. Further investigations on this topic are warranted.

The most unexpected finding of the present study was alteration of the ceramide composition in the cerebellum of APP<sup>SL</sup> mice, a brain region lacking A $\beta$  deposits and regarded as nonvulnerable to the disease. Intriguingly, we noted a significant increase of 2-HFA-ceramides (+50%) which was concomitant with a slight decrease in NFA-ceramides. However, considering the total ceramide content,

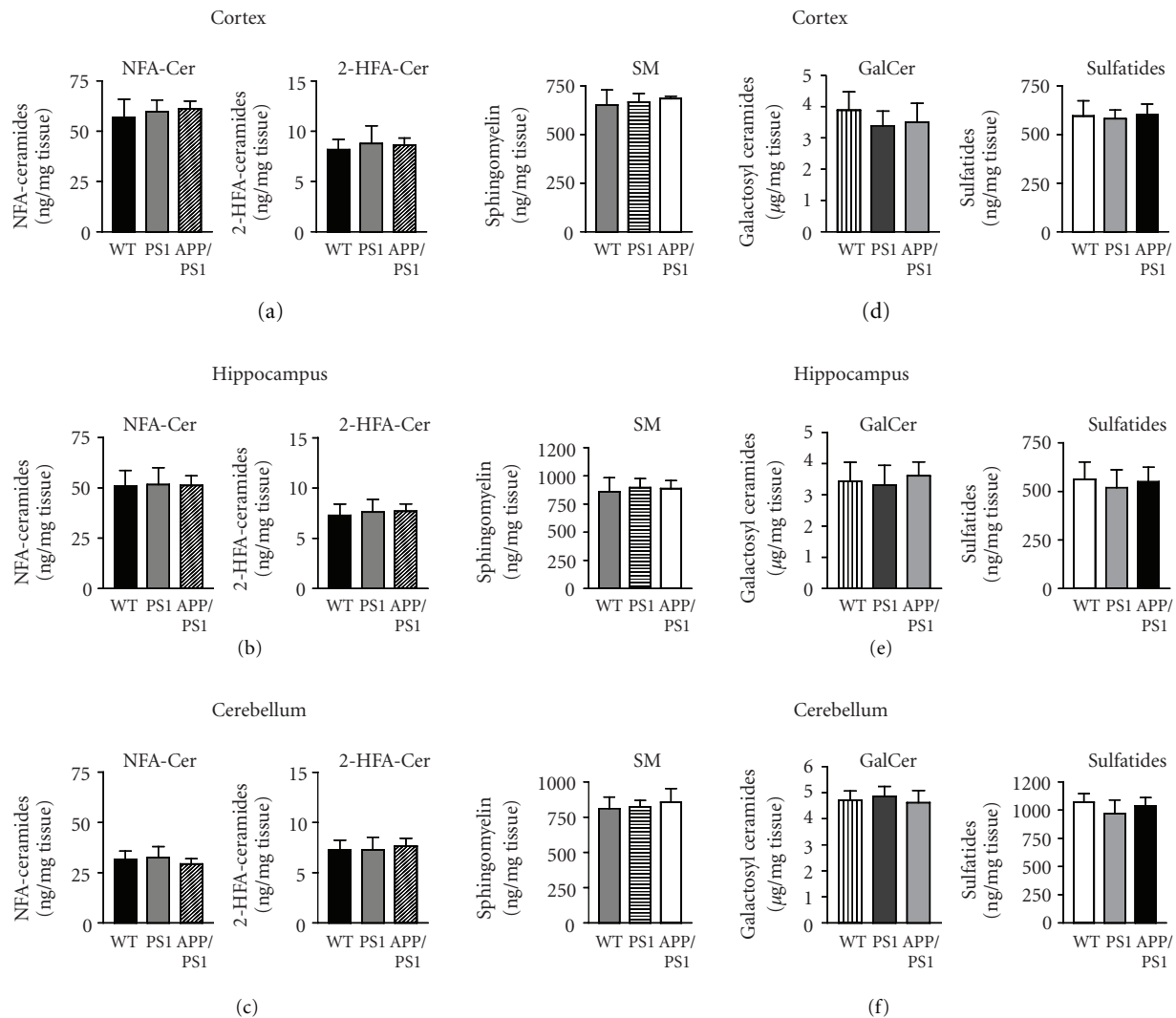


FIGURE 2: Levels of NFA-ceramides and 2-HFA-ceramides (a–c) and other related-sphingolipids (SM, GalCer, and sulfatides) (d–f) in the cortex, hippocampus, and cerebellum of 12-month-old APP<sup>SL</sup>/PS1<sup>M146L</sup>, PS1<sup>M146L</sup> mice, and age-matched nontransgenic mice. WT: wild-type control mice. Each sphingolipid class was analyzed by HPTLC and their respective concentrations were calculated from standard curves after densitometric scanning of the plates as described under Section 2. Values are expressed as the means  $\pm$  S.D. There was no significant difference in all sphingolipid levels between wild-type (WT), PS1<sup>M146L</sup>, and APP<sup>SL</sup>/PS1<sup>M146L</sup> mice in either cortex, hippocampus, or cerebellum (Dunn's multiple comparison test following a Kruskal-Wallis test).

it was almost similar between wild-type and APP<sup>SL</sup> mice. Previously, we found a more dramatic 161% increase of 2-HFA-ceramides in the cortex of APP<sup>SL</sup>/PS1Ki mice but contrary to the present results, it was accompanied by an elevation of NFA-ceramides.

Hydroxy FA-ceramides are relatively minor species of membrane lipids. As evident from the literature, the current knowledge about the metabolism and physiological function of 2-HFA-ceramides is very limited. In particular in AD studies, no attention was paid to 2-HFA-ceramides, rendering it very difficult to draw conclusions about the role of these ceramide species in AD physiopathology. Nevertheless, a couple of interesting facts suggest that these HFA species may participate to AD pathology: (i) it was recently found that A $\beta$  selectively bound to sphingolipids

that contained a 2-OH group on the ceramide backbone and did not effectively interact with sphingolipids that contained a nonhydroxylated fatty acid, favoring a conformational shift that disrupts membrane stability and promotes peptide-peptide interactions and oligomer formation [46]; (ii) the enzyme UDP-galactose: ceramide galactosyltransferase (CGT), which transfers galactose to both NFA- and 2-HFA-ceramides, was found to be upregulated in human AD brain [21]. Interestingly, overexpression of CGT in transgenic mice led to a reversal NFA : HFA-Galcer ratio which resulted in both decrease in HFA-Galcer and increase in NFA-Galcer levels [47]. Reducing the HFA-Galcer level would lead to an accumulation of their immediate precursors, 2-HFA-ceramides; (iii) there is some evidence for enhanced apoptosis-inducing activity of 2-HFA-ceramides compared

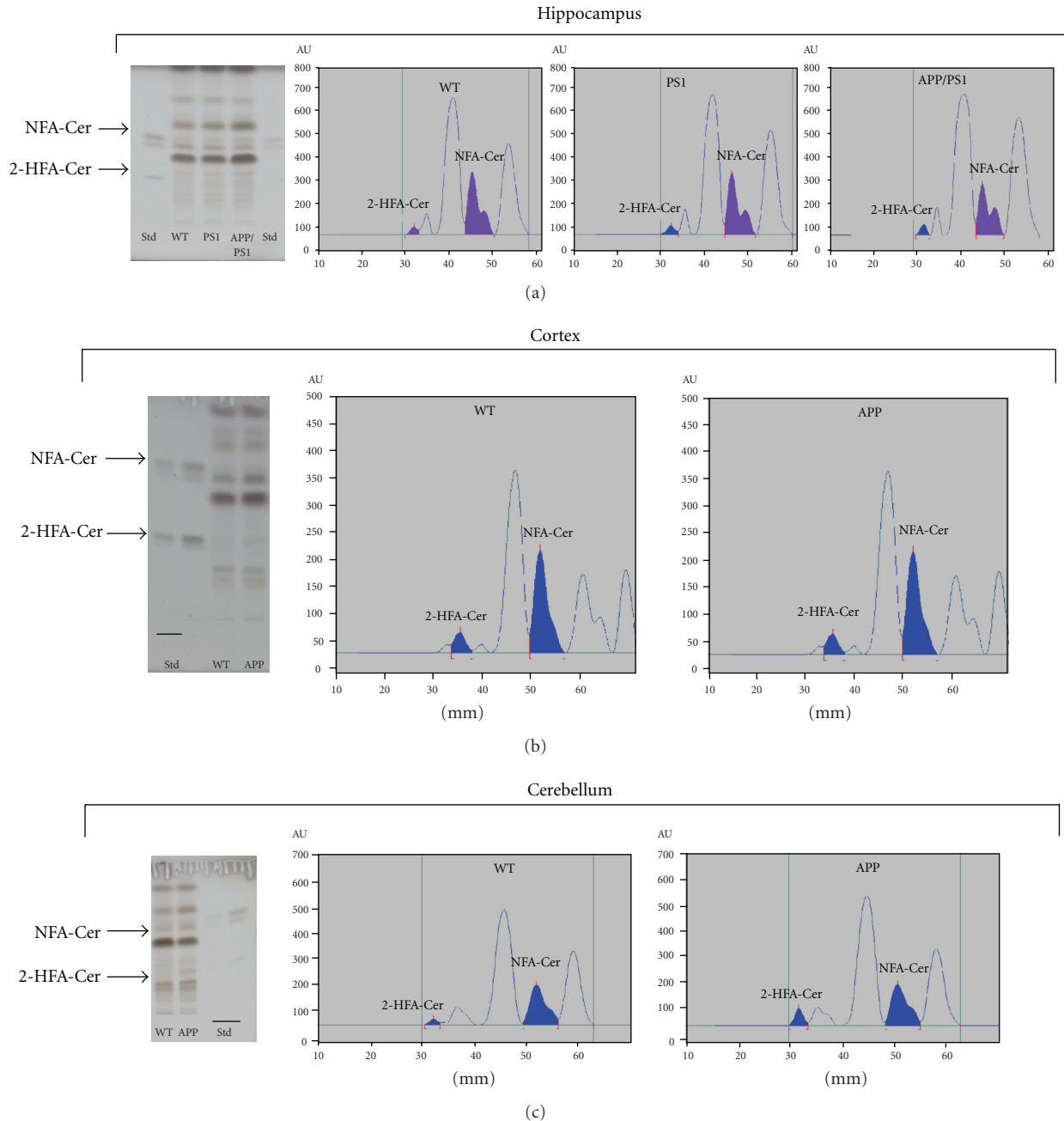


FIGURE 3: Typical HPTLC profiles of ceramides from hippocampus of 12-month-old APP<sup>SL</sup>/PS1<sup>M146L</sup>, PS1<sup>M146L</sup>, and their age-matched wild-type (WT) control mice (a), and from cerebral cortex and cerebellum of 24-month-old APP<sup>SL</sup> mice and age-matched WT control ((b) and (c), resp.). The densitometric analyses of the HPTLC plates were shown in parallel, respectively. Std: a mixture of standard NFA-ceramides and 2-HFA-ceramides. Ceramides were developed on HPTLC plates with chloroform-methanol (50:3) and located by spraying the plate with copper acetate 3% in H<sub>3</sub>PO<sub>4</sub> 8% reagent, followed by heating. Both 2-HFA-Cer and NFA-Cer appear as two bands corresponding to long-chain ceramides ( $\geq 22$ C; upper band) and short-chain ceramides ( $\leq 18$ C; lower band). Quantitative evaluation of ceramides was performed by scanning the plate at 396 nm with the Camag TLC Scanner 3/WinCats software system.

to NFA-ceramides [48], and this effect seems to be cell type specific. In this sight, mouse mutants with defective saposin D dramatically accumulate HFA-ceramides in cerebellum, resulting in a selective loss of cerebellar Purkinje cells [49]; (iv) we reported a gender-specific expression of HFA- versus NFA-ceramides in the APP<sup>SL</sup>/PS1Ki mouse model of AD,

and this biochemical feature could be related to the increase propensity of females to develop earlier neuronal loss [27].

Although the degree of 2-HFA-ceramide accumulation in the cerebellum of APP<sup>SL</sup> mice is much lesser than that seen in the cortex of the APP<sup>SL</sup>/PS1Ki mice, the reasons for these biochemical changes in this amyloid-free brain area

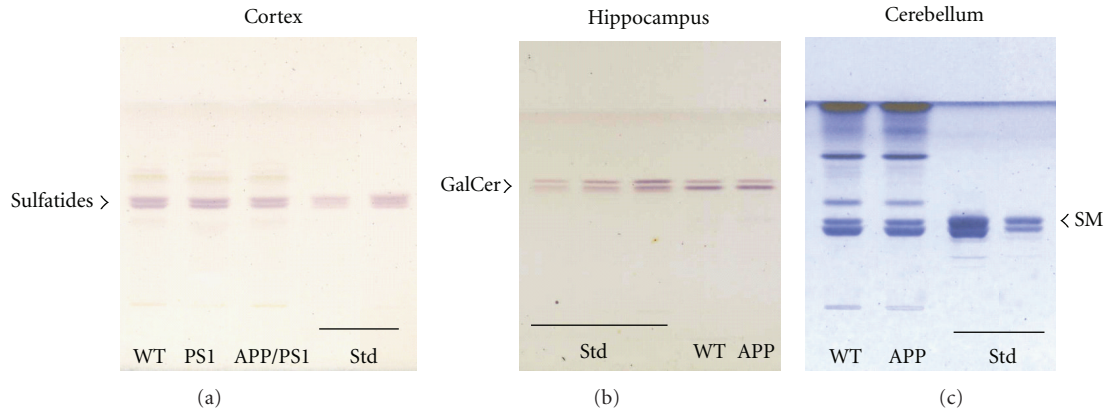


FIGURE 4: Examples of HPTLC profiles of sphingolipids from different brain regions of nontransgenic and transgenic mice. (a) Sulfatides from cerebral cortex of 12-month-old APP<sup>SL</sup>/PS1<sup>M146L</sup>, PS1<sup>M146L</sup>, and their age-matched wild-type (WT) control mice. (b) Galactosylceramides (GalCer) from hippocampus of 24-month-old APP<sup>SL</sup> mice and age-matched WT control mice. Galcer and sulfatides were developed in chloroform-methanol-water (65:25:4), sprayed with orcinol-H<sub>2</sub>SO<sub>4</sub> reagent, and then heated. Both Galcer and sulfatides\* appear as two bands corresponding to the 2-HFA- (lower band) and NFA-containing galactolipids (upper band), respectively. \*Standard sulfatides from bovine brain resolved in three bands, as a result of different fatty acid chain length. (c) Sphingomyelins (SM) from cerebellum of 24-month-old APP<sup>SL</sup> mice and age-matched WT control mice; SMs were developed with chloroform-methanol-water (60:35:8) (v/v/v) and visualized with sulfuric acid–CuSO<sub>4</sub>-ammonium molybdate spray reagent followed by heating. SMs appear as two bands which result of the differences in the fatty acid chain length. Std: standard sulfatides, GalCer, and SM, respectively.

are currently unknown. Possibly, it might reflect alterations of ceramide metabolism, since there is evidence that other metabolic pathways are perturbed in the cerebellum of these mice [50]. Hydroxy FA sphingolipids are synthesized by the same set of enzymes as nonhydroxy sphingolipids, except for fatty acid 2-hydroxylase (FA2H). The expression of FA2H is highly variable among cell types and is inducible by certain stimuli [48]. One may speculate that, upon unknown signal, 2-HFA-ceramides may be preferentially synthesized instead of NFA-species. Abnormal degradation of HFA sphingolipids may be also possible. It has been shown that galactosylceramidase, which forms 2-HFA-ceramides from Galcer is up-regulated, whereas acid ceramidase which hydrolyzed 2-HFA-ceramides into HFA and sphingosine is down-regulated in human AD brain [21]. Thus, with combinatorial up- and down-regulation of enzymes involved in sphingolipid metabolism, the cell could modify the levels of 2-HFA-ceramides in response to the changing cellular environment. However, this is highly speculative and further investigation is warranted to determine whether these factors or other unknown factors contribute to such changes of the ceramide profile in the APP<sup>SL</sup> cerebellum. It should be noted that also intriguing is the substantial elevation of ceramide reported by Han et al. [18] in the cerebellum of AD patients; this point also remains to be clarified.

In this study, we also examined the content of other ceramide-related sphingolipid classes including SM, Galcer, and sulfatides. Similarly to what we observed in the APP<sup>SL</sup>/PS1Ki model, we did not found any changes of SM and galactolipid levels in all brain regions from the two transgenic lines investigated. Similar findings were seen in APP<sup>sw</sup> and APPV717F transgenic mice, respectively, except for sulfatides [26]. Indeed, by contrast to our results, a loss

of sulfatide content was observed in multiple brain regions of these animals. The reasons for such discrepancies are still unclear, but it may be ascribed to the different genetic background of mouse lines and/or the genetic constructs based on different APP mutation and different promoters. Supporting this, it has been shown for example, that APP<sup>SL</sup> transgenic and wildtype mice on C57BL/6 background have lower basal cholesterol levels than the Ki mouse lines which are on C57BL/6 50%-CBA 25%-129SV 25% background [44]. Another example is the difference of lipid composition reported by Sawamura and coworkers [15] between mouse lines with C57BL/6J and FVB/N backgrounds, respectively. Moreover, these authors found that PS2 transgenic mice with C57BL/6J background displayed significant phospholipid alterations, particularly of SM, as compared to their wild-type controls, while PS2 transgenic mice with FVB/N background did not. These few examples point out the difficulties to compare the results from various mouse lines and reinforce the idea that additional studies in this field are required.

## 5. Conclusion

In summary, this study extends previous observations on sphingolipid alterations in animal models of AD. Despite several limitations, in particular the lack of old double transgenics, the present results demonstrated that, in the absence of neurodegeneration, no elevation of ceramides occurred in disease-affected brain regions from single APP<sup>SL</sup> mice, thus corroborating recent findings in two other single APP mice [26]. Moreover, since both neuronal loss and accumulation of toxic N-truncated A $\beta$  peptides are lacking in the APP<sup>SL</sup> model, this might suggest that A $\beta$ -induced

ceramide production is an important event leading to neuronal death. In the future, to support this hypothesis, it will be interesting to analyse the sphingolipid composition of the TBA2 mice, the new model expressing only N-truncated  $A\beta_{3(pE)-42}$  and which develops a severe neuronal loss [40], to evaluate whether or not ceramides, especially the 2-OH species, accumulate in the brain of these mice.

Accumulating and crossing the information obtained from various animal models will help to better understand the exact mechanism by which these sphingolipids contribute to AD pathogenesis.

## Abbreviations

AD: Alzheimer's disease  
APP: Amyloid precursor protein  
2 HFA: 2-hydroxy fatty acid  
NFA: Nonhydroxy fatty acid.

## Acknowledgments

The authors thank Laurent Pradier and Martine Latta-Mahieu from Sanofi-Aventis (Vitry sur Seine, France) for kindly providing the mice and Raymond Pontcharraud for his excellent technical assistance. This study was supported by the French Ministry of Education and Research, with a grant to the Research Unit GReViC, EA 3808, the University of Poitiers and CHU of Poitiers.

## References

- [1] S. Grösgen, M. O. W. Grimm, P. Frieß, and T. Hartmann, "Role of amyloid beta in lipid homeostasis," *Biochimica et Biophysica Acta*, vol. 1801, no. 8, pp. 966–974, 2010.
- [2] T. Hartmann, J. Kuchenbecker, and M. O. Grimm, "Alzheimer's disease: the lipid connection," *Journal of Neurochemistry*, vol. 103, pp. 159–170, 2007.
- [3] K. S. Vetrivel and G. Thinakaran, "Membrane rafts in Alzheimer's disease beta-amyloid production," *Biochimica et Biophysica Acta*, vol. 1801, no. 8, pp. 860–867, 2010.
- [4] Y. A. Hannun and L. M. Obeid, "The ceramide-centric universe of lipid-mediated cell regulation: stress encounters of the lipid kind," *Journal of Biological Chemistry*, vol. 277, no. 29, pp. 25847–25850, 2002.
- [5] M. Schenck, A. Carpintero, H. Grassmé, F. Lang, and E. Gulbins, "Ceramide: physiological and pathophysiological aspects," *Archives of Biochemistry and Biophysics*, vol. 462, no. 2, pp. 171–175, 2007.
- [6] G. Arboleda, L. C. Morales, B. Benítez, and H. Arboleda, "Regulation of ceramide-induced neuronal death: cell metabolism meets neurodegeneration," *Brain Research Reviews*, vol. 59, no. 2, pp. 333–346, 2009.
- [7] A. Morales, H. Lee, F. M. Goñi, R. Kolesnick, and J. C. Fernandez-Checa, "Sphingolipids and cell death," *Apoptosis*, vol. 12, no. 5, pp. 923–939, 2007.
- [8] B. J. Pettus, C. E. Chalfant, and Y. A. Hannun, "Ceramide in apoptosis: an overview and current perspectives," *Biochimica et Biophysica Acta*, vol. 1585, no. 2–3, pp. 114–125, 2002.
- [9] R. G. Cutler, J. Kelly, K. Storie et al., "Involvement of oxidative stress-induced abnormalities in ceramide and cholesterol metabolism in brain aging and Alzheimer's disease," *Proceedings of the National Academy of Sciences of the United States of America*, vol. 101, no. 7, pp. 2070–2075, 2004.
- [10] A. Jana and K. Pahan, "Fibrillar amyloid- $\beta$  peptides kill human primary neurons via NADPH oxidase-mediated activation of neutral sphingomyelinase: implications for Alzheimer's disease," *Journal of Biological Chemistry*, vol. 279, no. 49, pp. 51451–51459, 2004.
- [11] S. Chen, J. M. Lee, C. Zeng, H. Chen, C. Y. Hsu, and J. Xu, "Amyloid beta peptide increases DP5 expression via activation of neutral sphingomyelinase and JNK in oligodendrocytes," *Journal of Neurochemistry*, vol. 97, no. 3, pp. 631–640, 2006.
- [12] M. O. W. Grimm, H. S. Grimm, A. J. Pätzold et al., "Regulation of cholesterol and sphingomyelin metabolism by amyloid- $\beta$  and presenilin," *Nature Cell Biology*, vol. 7, no. 11, pp. 1118–1123, 2005.
- [13] L. Puglielli, B. C. Ellis, A. J. Saunders, and D. M. Kovacs, "Ceramide stabilizes  $\beta$ -site amyloid precursor protein-cleaving enzyme 1 and promotes amyloid  $\beta$ -peptide biogenesis," *Journal of Biological Chemistry*, vol. 278, no. 22, pp. 19777–19783, 2003.
- [14] S. Patil, J. Melrose, and C. Chan, "Involvement of astroglial ceramide in palmitic acid-induced Alzheimer-like changes in primary neurons," *European Journal of Neuroscience*, vol. 26, no. 8, pp. 2131–2141, 2007.
- [15] N. Sawamura, M. Morishima-Kawashima, H. Waki et al., "Mutant presenilin 2 transgenic mice: a large increase in the levels of  $A\beta_{342}$  is presumably associated with the low density membrane domain that contains decreased levels of glycerophospholipids and sphingomyelin," *Journal of Biological Chemistry*, vol. 275, no. 36, pp. 27901–27908, 2000.
- [16] I. Y. Tamboli, K. Prager, E. Barth, M. Heneka, K. Sandhoff, and J. Walter, "Inhibition of glycosphingolipid biosynthesis reduces secretion of the  $\beta$ -amyloid precursor protein and amyloid  $\beta$ -peptide," *Journal of Biological Chemistry*, vol. 280, no. 30, pp. 28110–28117, 2005.
- [17] C. G. Gottfries, I. Karlsson, and L. Svennerholm, "Membrane components separate early-onset Alzheimer's disease from senile dementia of the Alzheimer type," *International Psychogeriatrics*, vol. 8, no. 3, pp. 365–372, 1996.
- [18] X. Han, D. M. Holtzman, D. W. McKeel, J. Kelley, and J. C. Morris, "Substantial sulfatide deficiency and ceramide elevation in very early Alzheimer's disease: potential role in disease pathogenesis," *Journal of Neurochemistry*, vol. 82, no. 4, pp. 809–818, 2002.
- [19] J. W. Pettegrew, K. Panchalingam, R. L. Hamilton, and R. J. McClellure, "Brain membrane phospholipid alterations in Alzheimer's disease," *Neurochemical Research*, vol. 26, no. 7, pp. 771–782, 2001.
- [20] H. Sato, H. Tomimoto, R. Ohtani et al., "Astroglial expression of ceramide in Alzheimer's disease brains: a role during neuronal apoptosis," *Neuroscience*, vol. 130, no. 3, pp. 657–666, 2005.
- [21] P. Katsel, C. Li, and V. Haroutunian, "Gene expression alterations in the sphingolipid metabolism pathways during progression of dementia and Alzheimer's disease: a shift toward ceramide accumulation at the earliest recognizable stages of Alzheimer's disease?" *Neurochemical Research*, vol. 32, no. 4–5, pp. 845–856, 2007.
- [22] N. Marks, M. J. Berg, M. Saito, and M. Saito, "Glucosylceramide synthase decrease in frontal cortex of Alzheimer brain correlates with abnormal increase in endogenous ceramides: consequences to morphology and viability on enzyme suppression in cultured primary neurons," *Brain Research*, vol. 1191, pp. 136–147, 2008.

- [23] C. Duyckaerts, M. C. Potier, and B. Delatour, "Alzheimer disease models and human neuropathology: similarities and differences," *Acta Neuropathologica*, vol. 115, no. 1, pp. 5–38, 2008.
- [24] G. A. Higgins and H. Jacobsen, "Transgenic mouse models of Alzheimer's disease: phenotype and application," *Behavioural Pharmacology*, vol. 14, no. 5–6, pp. 419–438, 2003.
- [25] G. Wang, J. Silva, S. Dasgupta, and E. Bieberich, "Long-chain ceramide is elevated in presenilin 1 (PS1M146V) mouse brain and induces apoptosis in PS1 astrocytes," *Glia*, vol. 56, no. 4, pp. 449–456, 2008.
- [26] H. Cheng, Y. Zhou, D. M. Holtzman, and X. Han, "Apolipoprotein E mediates sulfatide depletion in animal models of Alzheimer's disease," *Neurobiology of Aging*, vol. 31, no. 7, pp. 1188–1196, 2010.
- [27] L. Barrier, S. Ingrand, B. Fauconneau, and G. Page, "Gender-dependent accumulation of ceramides in the cerebral cortex of the APPSL/PS1Ki mouse model of Alzheimer's disease," *Neurobiology of Aging*, vol. 31, no. 11, pp. 1843–1853, 2010.
- [28] C. Casas, N. Sergeant, J. M. Itier et al., "Massive CA1/2 neuronal loss with intraneuronal and N-terminal truncated A $\beta$  accumulation in a novel Alzheimer transgenic model," *American Journal of Pathology*, vol. 165, no. 4, pp. 1289–1300, 2004.
- [29] V. Blanchard, S. Moussaoui, C. Czech et al., "Time sequence of maturation of dystrophic neurites associated with A $\beta$  deposits in APP/PS1 transgenic mice," *Experimental Neurology*, vol. 184, no. 1, pp. 247–263, 2003.
- [30] C. Schmitz, B. P. F. Rutten, A. Pielen et al., "Hippocampal neuronal loss exceeds amyloid plaque load in a transgenic mouse model of Alzheimer's disease," *American Journal of Pathology*, vol. 164, no. 4, pp. 1495–1502, 2004.
- [31] S. Schäfer, O. Wirths, G. Multhaup, and T. A. Bayer, "Gender dependent APP processing in a transgenic mouse model of Alzheimer's disease," *Journal of Neural Transmission*, vol. 114, no. 3, pp. 387–394, 2007.
- [32] J. Wang, H. Tanila, J. Puolivali, I. Kadish, and T. Van Groen, "Gender differences in the amount and deposition of amyloid $\beta$  in APPswe and PS1 double transgenic mice," *Neurobiology of Disease*, vol. 14, no. 3, pp. 318–327, 2003.
- [33] L. Barrier, S. Ingrand, M. Damjanac, A. Rioux Bilan, J. Hugon, and G. Page, "Genotype-related changes of ganglioside composition in brain regions of transgenic mouse models of Alzheimer's disease," *Neurobiology of Aging*, vol. 28, no. 12, pp. 1863–1872, 2007.
- [34] S. Ladisch and B. Gillard, "A solvent partition method for microscale ganglioside purification," *Analytical Biochemistry*, vol. 146, no. 1, pp. 220–231, 1985.
- [35] V. V. R. Bandaru, J. Troncoso, D. Wheeler et al., "ApoE4 disrupts sterol and sphingolipid metabolism in Alzheimer's but not normal brain," *Neurobiology of Aging*, vol. 30, no. 4, pp. 591–599, 2009.
- [36] D. Z. Christensen, S. L. Kraus, A. Flohr, M. C. Cotel, O. Wirths, and T. A. Bayer, "Transient intraneuronal A $\beta$  rather than extracellular plaque pathology correlates with neuron loss in the frontal cortex of APP/PS1KI mice," *Acta Neuropathologica*, vol. 116, no. 6, pp. 647–655, 2008.
- [37] S. Oddo, A. Caccamo, J. D. Shepherd et al., "Triple-transgenic model of Alzheimer's disease with plaques and tangles: intracellular A $\beta$  and synaptic dysfunction," *Neuron*, vol. 39, no. 3, pp. 409–421, 2003.
- [38] O. Wirths, G. Multhaup, C. Czech et al., "Intraneuronal A $\beta$  accumulation precedes plaque formation in  $\beta$ -amyloid precursor protein and presenilin-1 double-transgenic mice," *Neuroscience Letters*, vol. 306, no. 1–2, pp. 116–120, 2001.
- [39] Y. Harigaya, T. C. Saido, C. B. Eckman, C. M. Prada, M. Shoji, and S. G. Younkin, "Amyloid  $\beta$  protein starting pyroglutamate at position 3 is a major component of the amyloid deposits in the Alzheimer's disease brain," *Biochemical and Biophysical Research Communications*, vol. 276, no. 2, pp. 422–427, 2000.
- [40] O. Wirths, H. Breyhan, H. Cynis, S. Schilling, H. U. Demuth, and T. A. Bayer, "Intraneuronal pyroglutamate-A $\beta$  3–42 triggers neurodegeneration and lethal neurological deficits in a transgenic mouse model," *Acta Neuropathologica*, vol. 118, no. 4, pp. 487–496, 2009.
- [41] T. A. Bayer and O. Wirths, "Review on the APP/PS1KI mouse model: intraneuronal A $\beta$  accumulation triggers axonopathy, neuron loss and working memory impairment," *Genes, Brain and Behavior*, vol. 7, supplement 1, pp. 6–11, 2008.
- [42] Y. M. Kuo, T. A. Kokjohn, T. G. Beach et al., "Comparative analysis of amyloid- $\beta$  chemical structure and amyloid plaque morphology of transgenic mouse and Alzheimer's disease brains," *Journal of Biological Chemistry*, vol. 276, no. 16, pp. 12991–12998, 2001.
- [43] A. Güntert, H. Döbeli, and B. Bohrmann, "High sensitivity analysis of amyloid-beta peptide composition in amyloid deposits from human and PS2APP mouse brain," *Neuroscience*, vol. 143, no. 2, pp. 461–475, 2006.
- [44] O. Wirths, K. Thelen, H. Breyhan et al., "Decreased plasma cholesterol levels during aging in transgenic mouse models of Alzheimer's disease," *Experimental Gerontology*, vol. 41, no. 2, pp. 220–224, 2006.
- [45] D. Z. Christensen, T. A. Bayer, and O. Wirths, "Intracellular A $\beta$  triggers neuron loss in the cholinergic system of the APP/PS1KI mouse model of Alzheimer's disease," *Neurobiology of Aging*, vol. 31, no. 7, pp. 1153–1163, 2010.
- [46] N. Yahi, A. Aulas, and J. Fantini, "How cholesterol constrains glycolipid conformation for optimal recognition of Alzheimer's  $\beta$  amyloid peptide (A $\beta$ <sub>1–40</sub>)," *PLoS One*, vol. 5, no. 2, Article ID e9079, 2010.
- [47] S. N. Fewou, H. Büssow, N. Schaeren-Wiemers et al., "Reversal of non-hydroxy:  $\alpha$ -hydroxy galactosylceramide ratio and unstable myelin in transgenic mice overexpressing UDP-galactose: ceramide galactosyltransferase," *Journal of Neurochemistry*, vol. 94, no. 2, pp. 469–481, 2005.
- [48] H. Hama, "Fatty acid 2-Hydroxylation in mammalian sphingolipid biology," *Biochimica et Biophysica Acta*, vol. 1801, no. 4, pp. 405–414, 2010.
- [49] J. Matsuda, M. Kido, K. Tadano-Aritomi et al., "Mutation in saposin D domain of sphingolipid activator protein gene causes urinary system defects and cerebellar Purkinje cell degeneration with accumulation of hydroxy fatty acid-containing ceramide in mouse," *Human Molecular Genetics*, vol. 13, no. 21, pp. 2709–2723, 2004.
- [50] C. Lafay-Chebassier, M. Paccalin, G. Page et al., "mTOR/p70S6k signalling alteration by A $\beta$  exposure as well as in APP-PS1 transgenic models and in patients with Alzheimer's disease," *Journal of Neurochemistry*, vol. 94, no. 1, pp. 215–225, 2005.

